International Conference on Space Optics—ICSO 1997

Toulouse, France

2–4 December 1997

Edited by George Otrio

The PRONAOS telescope

G. Serra, C. Sirmain, J. M. Lamarre, F. Buisson, et al.

International Conference on Space Optics — ICSO 1997, edited by Georges Otrio, Proc. of SPIE Vol. 10570, 1057012 · © 1997 ESA and CNES · CCC code: 0277-786X/18/$18 · doi: 10.1117/12.2326476

THE PRONAOS TELESCOPE

ICSO conference - 2 / 3 december 1997 - Toulouse (F)

G Serra[2], C Sirmain[1], J M Lamarre [3], F Buisson[1],

I Ristorcelli[2], J P Dinis[1], M Giard[2], F Pajot[3]

---

1 - Centre National d'Etudes Spatiales (e-mail contact sirmain@cnes.fr)

2 - Centre d'Etudes Spatiales des Rayonnements (e-mail contact serra@cesr.fr)

3 - Institut d'Astrophysique Spatiale (e-mail contact lamarre@ias.fr)

Abstract

PRONAOS is a stratospheric balloon borne experiment dedicated to astronomy in the sub-millimeter range

The scientific objectives are related to the improvement of our knowledge in the field of cosmology (using the Sunyaev-Zeldovitch effect measurements) and galactic physics (better understanding of some of the interstellar medium properties)

High performances were required for Pronaos both for instrumentation and the gondola specially the two meters telescope pointed at 20 arcsecs accuracy

In September 1996 the second flight was a success expected performances were confirmed and permitted to achieve the main objectives

A new kind of objects reflecting a very early stage of formation of stars were discovered The first detection of the positive part of the Sunyaev-Zeldovitch effect was performed

1. INTRODUCTION.

PRONAOS is conducted by CNES, with CESR for science management and IAS taking in charge the instrument The PRONAOS program is a French achievement, designed and built in a large national cooperation, between CNES and various CNRS laboratories

What makes it original is the difficulty of the scientific objectives in terms of sensitivity, implying high performances, which led to a sophisticated design, making PRONAOS have many things in common with a satellite

A first flight was realized in September 1994 it permitted to verify the ability of the system to achieve its requirements and brought the first scientific results, even if these one were limited, due to failures which restricted the duration of observations A second flight was conducted on September 22[nd] 1996, from Fort-Sumner (New-Mexico) and was a full success

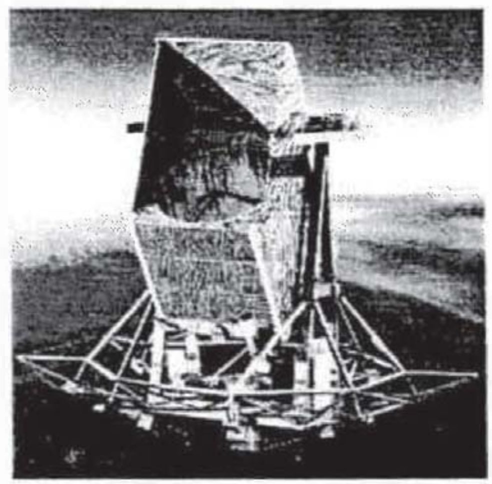

Figure 1 PRONAOS artist view

2. THE PRONAOS PROGRAM.

2.1 SCIENTIFIC OBJECTIVES.

The submillimeter (sbmm) range is one of the few regions of the electromagnetic spectrum which remains mostly unexplored in astronomy, because of the attenuation of the Earth atmosphere at these wavelengths and also because of the technological

1

difficulties associated to the detection However, this spectral range is of great importance both for galactic interstellar matter and cosmological studies The focal instrument accommodated on PRONAOS is a multiband photometer called SPM, designed for measurements ranging from 180μm to 1200μm, using direct detection

Several scientific objectives are devoted to PRONAOS-SPM The first class priority is the detection of the positive part of the Sunyaev-Zeldovitch effect on clusters of galaxies This effect results from an interaction between the cosmic background photons with intergalactic relativitc electrons, producing a spectral distorsion inside the cosmic blackbody radiation Another important objective is the measurement of the extended emission of the interstellar medium PRONAOS-SPM is designed to be very sensitive to low brightness gradients, in the sbmm range, allowing the observation of the cold dense cores inside the star forming regions

2.2 MISSION REQUIREMENTS.

These scientific objectives imply to operate at altitudes where the atmosphere is very transparent and shows a low emissivity PRONAOS has been designed to fly at ceiling altitudes of around 4 mbar (38 km) in the stratosphere.

Figure 2 PRONAOS Launch

The minimum altitude requirement has two fundamentals

- transmission budget for the instrument (acceptable in fact up to 10 mbar)
- ability of the pointing system to compensate the torque due to the aerodynamic pressure on the telescope (surface of 4 m²)

The mission requirements have been expressed in terms of minimum and desired values

Performance	Minimum	Desired
Flight Altitude	6.5 mbar (33 km)	4 mbar (38 km)
Flight Duration	14 hours	> 20 hours
Sensitivity (NEB)	10 MJy sr⁻¹ Hz⁻¹/²	<4 MJy sr⁻¹ Hz⁻¹/²
Pointing Stability	5″	5″
Pointing Precision	1′	20″

Table 1 Mission requirements

$1 MJy = 10^{-20} W m^{-2} Hz^{-1}$

2.3 MISSION DESCRIPTION.

2.3.1 Operational conditions.

The requirement of long duration flight (more than 20 hours at cruise altitude) implies to launch during turn-around period, that is the time of the year during which stratospheric winds which usually blow at speeds up to 100 knots progressively slow down and change direction (East - West) These phenomena last about 10 days and occur at the latitude of New-Mexico at the beginning of May and end of September The flight duration is then limited by to RF direct visibility, authorized flight area and consumables (ballast, energy, cryogenic liquids) Launch is also very constrained by local weather conditions

Balloon	1.1 Mm³ Open type Inflated with Helium
Parachute diameter	48 m (159 ft)
Total height	≈ 300 m
Total weight	≈ 5600 kg
Ballast	900 kg
Gondola	
dry mass	2050 kg
dimensions	8m x 7m x 7m
Telescope	
Diameter	2 m
Elevation range	20 ° to 60°

Table 2 System main characteristics

Operating such a system requires various specific facilities (large buildings, launching vehicle, launch pad, weather station, TM/TC station,). Such a facility is today available at the site of NASA in Fort-Sumner (New-Mexico) The US middle west desert is particulary convenient for this activity

2.3.2 Flight scenario.

During ascent, the gondola is passive. Stabilization is started upon arrival at ceiling and the telescope is unstowed.

The gondola and the payload are then directed to the direction of the Polar star, using a magnetometer and inclinometers. Inertial guidance is then started.

The telescope is then directed by inertial guidance to the submillimetric direction (azimuth swivel and elevation motors). The star sensor is directed with its pointing mechanism towards the pre-chosen star giving the inertial direction. The inertial guidance unit is giving instantaneous direction between two successives star sensor acquisitions. The different observation have a duration between a few minutes and 2 hours.

Flight termination is triggered from the ground when a safe place is anticipated for landing. The telescope is first stowed and locked in safe configuration and the equipments are switched off. The gondola is recovered underneath a parachute.

Operation	Duration
Launch preparation	14 hours
Launch operations	2 hours
Drive-up	2.5 hours
Float	29 hours
Descent	¾ hours
Recovery	8 hours

Table 3 Duration of mission phases (as experienced during Flight 2)

2.4 SYSTEM DESCRIPTION.

The gondola consists of three main sub-systems:
1) the service platform.
2) the telescope.
3) the focal instrument SPM.

The system also includes the ground to operate the gondola and perform real time analysis of the collected scientific data.

A detailed description of the system and the development is given in [Ref 1]. Also the [Ref 2] explains the pointing sub-system in great details. Concerning the flight softwares and the ground system, informations can be found in [Ref 3] and [Ref 4].

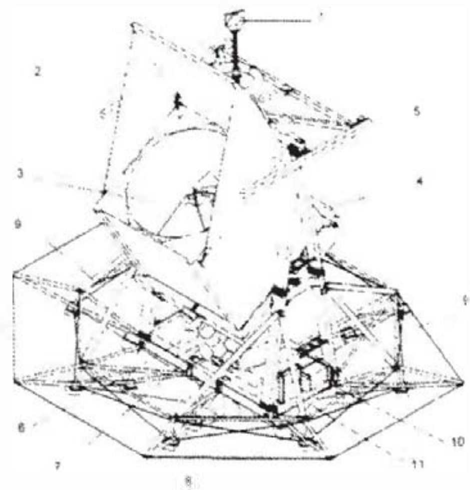

1 - Connection to balloon
2 - Telescope shutter
3 - Telescope
4 - Gimbal
5 - GPS antenna
6 - Li Batteries
7 - Star Sensor
8 - Main crush pad
9 - Landing structure
10 - TM TC Electronics
11 - Ballast hopper
12 - Azimuth swivel
13 - Swinging dampers
14 - Equipment Box

Figure 3 PRONAOS gondola

2.4.1 The SPM instrument.

The multi-channel photometer SPM has been described in detail in [Ref.5]. It consists mainly of two parts: 1) warm devices involving optics that ensure beam switching and in-flight calibration, electronics for housekeeping and data handling, and 2) a liquid helium cryostat containing optics, filters, ^3He refrigerators and four bolometers cooled at 0.3K. It weights 165 kg.

3. THE PRONAOS TELESCOPE.

3.1 THE TELESCOPE DESIGN

The PRONAOS telescope was manufactured by Matra Marconi Space in Toulouse. A detailed description of the telescope is given in [Ref. 6].

The optical design results from a compromise between:
- the scientific requirements asking both for a collecting area as large as possible and for a high spatial resolution,

- the constraints concerning the weight and dimensions of the gondola

An axi-symmetric Cassegrain configuration opened at F/10 has been chosen with a two meters segmented and active primary mirror.

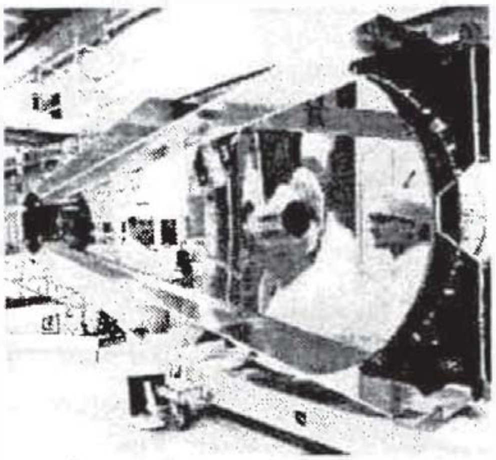

Figure 4 : Telescope during integration

The main mirror

The main mirror (M1) is made up of 6 identical light-weight segment mirrors (10 kg/m²). Each segment is manufactured by a replica process on a zerodur mold (made by REOSC) on a structure of honeycomb and skins in carbon fiber. The reflecting side is covered by a layer of epoxy resin and a reflective gold coating (150 nm thickness).

Type	Axi-symmetric Cassegrain
Focal length	20 m
Aperture ratio	f/10
Primary-secondary distance	1528.2 mm
Primary mirror - focal length - diameter - central hole diameter - weight	 1778.8 mm 2045 mm 255 mm [illegible] kg
Secondary mirror - focal length - diameter - reflecting central cone	 275.1 mm 277 mm ∅50 mm, h=4 mm
Total weight	225 kg

Table 2 : Telescope characteristics

The surface accuracy is around 1.9 µm rms regarding the best fit parabola and 2.7 µm rms with respect to the nominal profile. The position of each mirror is controlled by 3 actuators (electrical screw-jacks) with a 0.1 µm resolution and 5 capacitive sensors. Four sensors measure the distance between one point of the considered mirror and a reference plate supposed to be perfectly rigid. The fifth sensor located at the edge of each mirror gives the relative positioning between two adjacent mirrors. This active servo-loop allows to compensate for the temperature and gravity effects all along the flight.

The goal of PRONAOS is to make very sensitive measurement of brightness gradients. A significant effort has been done to decrease the various sources of noise encountered in submillimetre photometry.

Figure 5 : Telescope CAD view (integrated configuration)

The telescope has been designed to have the lowest possible thermal emission in order to reduce the noise induced on the detectors. This is achieved by avoiding any black item in the beam. The central hole of the Cassegrain primary mirror is not seen by the instrument thanks to a little cone put at the centre of the secondary mirror. The legs of the spider supporting the secondary are V shaped and coated with reflective materials. The cylindrical baffle is reflective in the submillimetre range. These choices are made with a the risk of increasing the straylight and only flight data have proved that this choice was the good one.

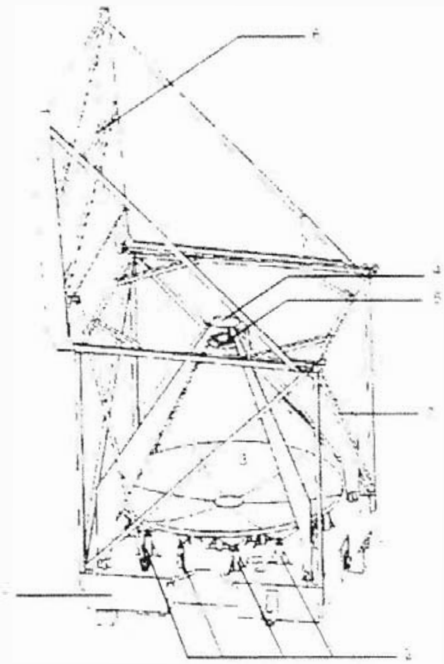

Figure 6 The 2 meter Telescope

3.2 THE OPTICAL SIZING.

The 2 m class telescope allows to obtain angular resolutions similar to those of the satellite IRAS at shorter wavelengths (5 to 10 times). The beam diameters in the four channels of the photometer SPM are given in the table 5.

They are oversized comparatively to the diffraction limit set by the telescope. The angular resolution (beam size) has been defined accounting for the uncertainties on other system parameters. They are scaled to include a source even in the case of a degraded pointing accuracy.

Band	Wavelengths (µm)	Beam size (FWHM)
1	180-240	2'
2	240-340	2'
3	340-540	2.5'
4	540-1050	3.5'

Table 5 Definition of bandwidths and beam sizes

The wavefront error results from a trade-off between the constraints related to the development of a new technology for the primary mirror (M1) of the telescope and the need for angular resolution at short wavelengths. Its RMS value has been set to 42µm with a goal of 30µm. This corresponds to a minimum wavelength for diffraction limited operation of 540µm and 390µm respectively (Marechal criterion).

ITEM	WFE_{rms}(µm)
Mirrors manufacturing	5.4
Mirrors stability to thermal effects	12
Effects of gravity variation	4
Fixation rigidity	1
Structure stability	0.2
On-ground mirrors alignment	22
Servo-control accuracy	8
TOTAL PRIMARY MIRROR (rms)	33
Secondary mirror manufacturing	3.4
Telescope global alignment	0.1
In-flight stability	4.6
TOTAL TELESCOPE (rms)	37

Table 6 Telescope WFE Budget

The sky chopping implemented by a wobbling mirror in the warm optics of SPM induces a movement of the beam with an amplitude of a few cm on the primary mirror. In consequence the synchronous detection of the photometric flux amplifies, together with the astronomical signal, the difference of the thermal emissions between the two edges of the M1. Therefore a temperature uniformity better than 1 degree is required across M1. A good thermal insulation from outside is implemented to reach this requirement. In addition, a cylindrical baffle, reflective in the submillimetre range, and thermally emissive makes an additional shield.

3.3 Telescope pointing requirements.

The pointing requirements are justified as follows

- pointing accuracy is justified by the acceptable flux loss associated with a bias between the object observed and the sensitive axis
- pointing stability is justified by the noise associated with the displacement of the source in the field

Considering that the instrument beam and source produces an illumination on the focal plane are gaussian, the collected energy ratio is

$$R(r_0) = \frac{E(x_0, y_0)}{E(0,0)} = e^{-\frac{r_0^2}{a^2+\varepsilon^2}}$$

with $r_0 = \sqrt{x_0^2 + y_0^2}$ the bias

a the radius of the beam

ε the radius of the image

We tolerate a flux loss smaller than 10%. With the assumption of the image having the same size as the beam, we got the following limits for the 4 bands (plus 1 band for future improvement of the system)

Band	1	2	3	4	Future
Beam Size	2	2'	2.5	3.5	1'
Precision	39"	39"	49"	68"	20"

Table 7 Pointing requirements

From which we established the pointing precision requirement of 20" (objective), and 1' (minimum) based on the value obtained on band 4, associated with the main objective (furthermore, the objects observed in bands 1, 2, 3 are usually large)

3.4 Telescope Alignments

Telescope alignment applies to the 6 segments forming the primary mirror, in order to set a reference position for the servo loop

Each segment mirror of the primary mirror presents 3 degrees of freedom

- - 2 rotations
  - β around a radial direction
  - ϕ around a direction perpendicular to the previous one in the same plane
- - 1 translation along the telescope axis

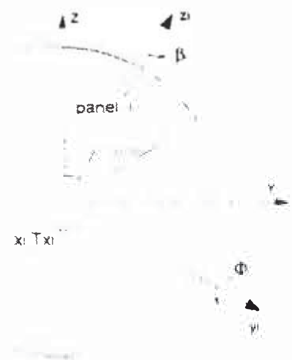

Figure 7 The segmented primary mirror and the mirrors degrees of freedom

Safa [Ref.9] has shown by modeling that the image quality was drastically dependent on the wavelength range of the incident radiation field. This is due to the spatial frequency of the surface defaults: it corresponds to λ/15 in the submillimeter and 24 λ in the visible. In consequence, the visible image energy distribution is limited by the diffusion, while it is diffraction limited in the submillimeter range

In particular, using its modeling, Safa [Ref 10] has shown that the diffusion image (visible) is not modified within a wide range of translation misalignment; on the contrary, at submillimeter wavelength, it can degrade considerably the diffraction image quality, because of interference effects

In consequence, the mirrors translation alignment had to be achieved in the submillimeter range.

However, it was possible to obtain the alignment of the mirrors tilts in the visible wavelength. Since the development of an experiment is much less constrained in the visible than in the Sbmm, we have decided to proceed in two stages: first, we have achieved the tilts alignments in the visible range, and then completed with the alignment in translation along the optical axis

To perform the rotation alignments, we used an autocollimation process in the visible range with the purpose to analyze the diffusion image associated with each mirror in the focal plane and to get it centered on the nominal focus position by means of its tilts movement (β, φ)

The precision obtained for this rotation control was estimated to be better than ±10"

The principle of translation positioning along the optical axis is to analyze the distortion of the diffraction image associated with a point source when the translation step varies between adjacent mirrors. We had to use a large wavelength passband incident beam, in order to break by the superposition of the different wavelengths the periodicity associated with a monochromatic beam (uncertainty of positioning at λ/2).

The source used is a high pressure mercury vapor arc lamp, which radiates both in the visible and the Submm, as an equivalent blackbody at a temperature T≈1800K, refocused by a parabolic mirror onto a hole source (Ø=1.3mm), modulated by means of a chopper and then placed at the focus point of a collimator (Ø=200mm), in order to obtain an output parallel beam. The detector we used is a silicium bolometer cooled at liquid helium temperature (T≈ 4K).

The diffraction image in the focal plane is obtained by moving the hole source in the collimator focal plane. After analysis of the diffraction image, the mirror is translated if needed of the calculated value by means of the three actuators (see figure 8).

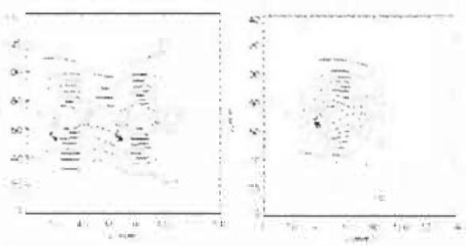

Figure 8 : Submillimetric diffraction image of sub-pupil F 200, located on 2 adjacent petals
Left : before alignment (50 µm gap)
Right : after petals alignment (7µm gap)

The image distortion is detectable by this method within ±7µm around the nominal translation position. An analysis of the diffraction images obtained for different positions of the sub-pupil along the intersegment has also allowed to improve the tilts control accuracy to ±8". We have deduced from these results the corresponding wave front error value: WFErms=22 µm.

3.5 PAYLOAD ALIGNMENT CONTROL

This operation permits to identify the axis of the Telescope associated with the instrument. The payload axis may be different from the nominal axis, mainly because of the optics alignment inside the focal instrument and a slight structure deformation due to the different mass configuration of this integrated system.

The method developed and applied for SPM is described in detail [Ref 8]. It consists in mapping the SPM response when a telescope sub-pupil is enlightened with a collimated beam which direction is scanned around the nominal telescope axis, using the same tool. The barycenter position is computed and allows to deduce the corresponding axis, measured by means of theodolites with respect to the telescope reference cube.

4. INFLIGHT RESULTS

4.1 LAST FLIGHT.

Flight 2 was performed on September 22 and 23, 1996. Throughout the 29 hours at float, 50 observations of sky regions were carried out.

Figure 9 displays the trajectory of the balloon, compared with the authorized flight area. This trajectory is very typical of a turn-around flight, the direction of the balloon changes with time and altitude and the position remains very close from the launch site.

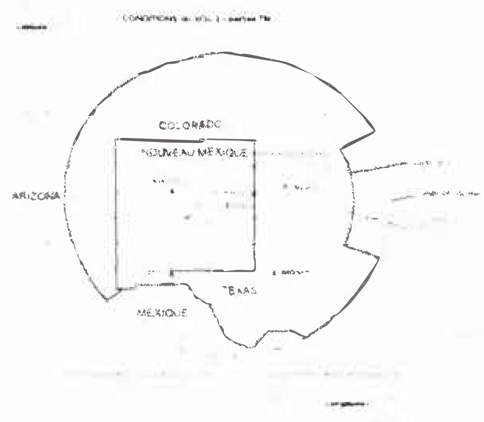

Figure 9 : Balloon trajectory vs authorized flight perimeter

Figure 10 displays the altitude of the balloon. On the first day, the balloon reached the altitude of 37.8 km/ 4 Hpa, it went down to 5.9 Hpa, that is 34.9 km during the night. On the second day, the balloon reached 3.5 Hpa / 38.7 km (higher than first day, since ballast had been dropped during the night).

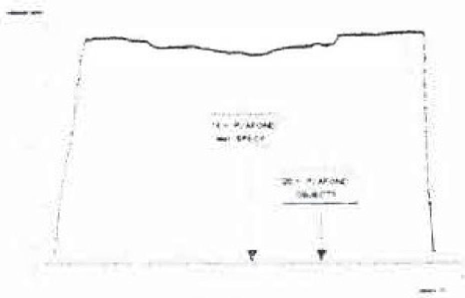

Figure 10 Balloon altitude

4.2 Technical results

4.2.1 Stabilization and pointing.

After reaching float, the amplitudes of the residual movements decreased. These movements were easily coped with by the stabilization system.

During flight, in several cases, the pointing system was not able to work properly and obliged an interruption of the observations:

- at night-day transition: this is probably due to the rapid ascent of the balloon, crossing layers of scattered winds, and maybe also to the change of shape of the balloon in relation with the change of volume.
- when the altitude became lower than 34.2 km, corresponding to a pressure higher than 5.7 Hpa. In this case the aerodynamic perturbation torque became too strong and beyond the capacity of the pointing system.

These cases represent a very short part of the flight (about 10%). The table 8 compares the performances of the pointing system as specified and as measured during the flight.

The values which are presented result from calculations made from the 50 scientific observations performed.

Misalignment between payload and star sensor is affected both by gravity (varying with elevation) and by thermal effects and is quite difficult either to be modeled or to be measured on ground. That bias was then regularly measured during the flight (20" in average).

These performances were convenient to guarantee a successful flight. In fact, most of the observations conducted were cartographies which were not so demanding in term of pointing precision. For the observations which really needed high precision pointing, we performed an alignment calibration prior to the observation, every time this was possible.

	Specif	Worst case	Average
Crude stabilization	2'	3.5'	1.2'
Pointing stability (short term)	2"	2"	0.5"
Pointing stability (over 1 observation)	28"	1.3'	20"
Absolute precision	60"	50"	20"

Table 8 Stability and pointing precision

4.2.2 Radiometry

Image quality

The observation of Saturn allowed to check the image quality of the telescope. This planet can be considered as an extended source but quite smaller than the beam size. It is also bright enough to give an excellent signal to noise ratio even in the far wings of the beam. The amplitude distribution allows to estimate the wavefront error (WFE) to 33µm RMS, which is inside the requirement, and not far from the goal.

Sensitivity

This good efficiency of the telescope and its low emissivity allowed to reach the expected sensitivity, or even a little better one. The next table gives the sensitivity to Rayleigh-Jeans brightness temperature in one second of integration time.

Channel	1	2	3	4
Sensitivity ($\mu K s^{1/2}$)	180	280	140	250

Table 9 Measured sensitivity

The sensitivity proved to improve as the square root of the integration time in channels 3 and 4, while it improved more slowly in channels 1 and 2, which is a sign of a non stationary noise in these channels that can be attributed to atmospheric noise or residual parasitic modulated fluxes.

4.3 Scientific results

4.3.1 Interstellar matter

Submillimeter is the unique wavelength range allowing the measurement of the whole temperature range of the grains including the cold component and then to have direct access to the whole dust mass and to the morphology of molecular clouds (condensations fragments filaments). Futhermore this spectral range is appropriate to study the opacity and physical properties of grains, key parameter to the understanding of star formation processes. During the PRONAOS flights, we mapped different sites of the interstellar medium star formation regions in Orion, Rho Ophucus, and M17 quiescent molecular clouds in Cygnus and Serpens Polaris Cirrus (diffuse clouds at high galactic latitude). The high sensitivity of SPM has allowed to detect very low brightness gradients emission (0.3 MJy/sr arcmin[1] for Δt= 1s at λ=600µm). From the simultaneous measurement of this emission within the four wavelength bands of SPM we deduced the averaged temperature and emissivity coefficient of the grains. Very cold condensations have been discovered with a respective typical temperature and size T=12 ± 2K, (l=0.1 to 1 parsec). These parameters together with dust models allow us to determine the density and mass of each object: it is found to vary from 1 to 40 solar masses. The prototype of such cold condensations is the « small cloud » discovered in the Orion Nebula during the first flight [Ref 7]. During the second flight, we observed three similar cold cores in the central part of the Ophiucus complex which is one of the nearest molecular cloud with an efficient star formation activity (see figure 11).

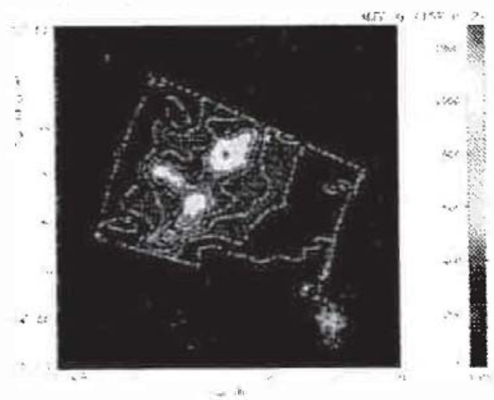

Figure 11 : Observation performed in the Rho-Ophiucus region

Under a well known young star at the top of the picture it reveals an unknown object at a very early stage of formation of star (before proto stellar formation). Its mass is about 12 times the sun mass and its dimension about 0.5 parsec.

The recent near infrared observations performed with ISO in this area show that two of these clumps were seen as sharp and deep absorption features against the diffuse cloud background at 5-6 µm. The comparison of the infrared absorption of the grains and their emission in the submillimeter range measured with PRONAOS allows to constrain the extinction curve of dust in this medium. The analysis of the cold condensations observed for the first time with PRONAOS is unique for constraining the star formation model.

4.3.2 Sunyaev-Zeldovitch Effect.

The Sunyaev-Zeldovitch (« SZ ») effect on clusters of galaxies results from Inverse-Compton interactions between the cosmic background photons with intergalactic relativite electrons. These interactions produce a spectral distorsion inside the cosmic blackbody radiation, with a brightness enhancement in the submm range (positive part of the SZ effect) and a lower level in the millimeter range (negative part). Using ground based radiotelescope, several groups have now detected the negative part of the SZ effect on some clusters of galaxies. But, up to PRONAOS-SPM, it was not possible to detect the positive part. To reach such a measurement, it is necessary to use very sensitive and accurate pointed space borne instrumentation. The first detection of the positive part of the SZ effect, was the main objective of the PRONAOS-SPM project.

Four clusters of galaxies were observed during the second PRONAOS-SPM flight. Two of them were observed in nominal conditions, with total integration time reaching two hours per each. For the cluster A478 his location, at rather low galactic latitude induces a detection perturbated by galactic dust emissions preventing a clean measurement of the SZ positive part. For the cluster A2163 a significant brightness excess was measured in the his direction in both bands 3 and 4. The unexpected excess in band 3 can be interpreted by comparing the PRONAOS-SPM observation to complementary measurements we have made at shorter wavelength using ISO (see figure 12).

The relative brightness observed in the direction of the cluster (in respect to the average surounding sky) can be interpreted by the addition of two components the SZ effect and a residual dust emission. So, with PRONAOS-SPM the first detection of the positive part of the SZ effect has been made.

---

[1] 1MJy = 10^{-20} W m^{-2} Hz^{-1}

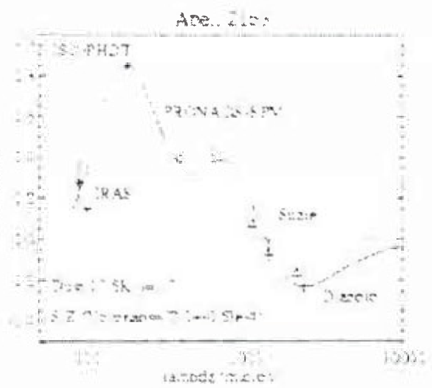

Figure 12: First observation of SZ

5. CONCLUSION

PRONAOS is today the only operational space system in the sub-millimetric range with such performances. It has demonstrated that unique scientific objectives could be reached with an instrumentation in stratospheric flight, at the price of important efforts.

The data obtained during flight 2, in conjunction with data obtained from a satellite (ISO) and ground observation, have permitted to produce major scientific results for the understanding of the evolution of the universe: in particular the first measurement of the positive part of the Sunyaev-Zeldovich effect. Futhermore, cold interstellar condensation were discovered in molecular clouds of our Galaxy.

High pointing performances have been reached, although they remain much dependent on the actual flight environmental conditions.

A third flight is currently under preparation. Its objectives will be to refine and complete the results already obtained: research of cold condensations in other parts of the galaxy, and in particular in high latitude cirrus, and improvement of the statistics on the S-Z effect.

These results, as well as the know-how acquired by the French community in the various technological developments, reveal to be precious for the preparation and the definition of future missions such as PLANCK SURVEYOR and FIRST.

References

[1] BUISSON and al. « The PRONAOS project: design, development and inflight results». IAF Turino Oct. 1997

[2] BERRUYS S., LEDU M., ROBERT A.
« The PRONAOS pointing and stabilization system ». 3rd ESA international conference on spacecraft guidance, navigation and control system, ESTEC Nov. 26-29 1996

[3] LAURENS A.
« PRONAOS flight software: a real-time application for a balloon-borne scientific gondola » in procedings of « Systemes informatiques temps reel pour les applications spatiales » Nov. 1992, Editions Cepadues (Toulouse, France)

[4] LAURENS A.
« PRONAOS ground control center: first operational Ada application in CNES » in proceedings « Ada in Europe 95 » 1995 Ed. Springer-Verlag (Germany)

[5] LAMARRE J.M. et al
1994 IR Phys. Tecno., Vol 35, N● 2/3, pp277-289

[6] BUISSON F. AND DURAN M.
1990 Proc. 29th Liege International Astrophysical Colloquium "From Ground-Based to Space-Borne Submillimeter Astronomy" Liege, Belgium, 3-4 July 1990 ESA SP 314 (December 1990)

[7] RISTORCELLI I et al
ApJ 1997 to be published

[8] RISTORCELLI I. et al
« The PRONAOS sub-millimeter semi-active Telescope » Journees Internationales de Nice sur les Antennes, Nice, Nov. 1996

[9] SALTH
Applied Optics, Vol. 31, N° 13, 1992

[10] SALTH
Ph. D. Thesis, 1991, CESR Toulouse, France

[11] HARPER D.A. et al
Astrophysical Journal, 1974, ApJ 192, 557